


 Cite this: *RSC Adv.*, 2026, 16, 18952

# Catechol-derived propargyl diol cyclizations with malonyl dichloride: substituent effects on the formation of macrocyclic esters and their hydrochlorinated adducts

 George Lefkaritis, <sup>a</sup> Andreas Kourtellaris, <sup>ab</sup> Nikos Chronakis<sup>†a</sup> and Savvas N. Georgiades \*<sup>a</sup>

A series of catechol-derived propargyl diols were synthesized in the current study, and submitted to cyclization with malonyl dichloride, under basic conditions, to afford the corresponding 13-membered macrocyclic diesters. Product distribution appeared to be associated with the choice of protecting group for the catechol hydroxy substituents. Diverse protecting groups, able to fine-tune the (stereo)electronic contribution of each substituent to the  $\pi$ -conjugated system were investigated. In the cases of a trifluoromethanesulfonate-substituted or a conformationally-restricted cyclohexyl dioxolane-comprising propargyl diol substrate, as well as the O-substituent-free propargyl diol counterpart, the reaction led to the expected macrocyclization, alongside traces of a 26-membered macrocyclic tetraester, without any indication of a competing hydrochloride addition to a propargyl triple bond. However, upon switching to silyl or methyl groups as catecholic O-atom protecting groups, hydrochloride addition occurred on a triple bond under the cyclization conditions, leading to formation of macrocyclic, vinyl chloride adducts, along with the expected intact 13-membered macrocycle. In either case, no metal catalysis was required, while the reaction was performed at ambient temperature. Control experiments involving alternative conditions and hydrochlorination agents, which may form *in situ* in the original reaction, were conducted, to provide insight on mechanistic aspects.

Received 25th November 2025

Accepted 27th March 2026

DOI: 10.1039/d5ra09108j

[rsc.li/rsc-advances](https://rsc.li/rsc-advances)

## Introduction

Macrocyclic esters are key structural motifs, both in Nature and in organic synthesis, as they can serve as scaffolds with unique 3D conformations, able to organize diverse substituents, in orientations that allow them to interact with target (bio)molecules or ions, or even template formation of supramolecular structures. In Nature, macrocyclic esters are mainly derived from intramolecular cyclization of a (polyketide or terpenoid) biosynthetic precursor, and referred to as macrolactones. Macrolactones are widely encountered in bacteria (*e.g.*, erythromycin series antibiotics), fungi (*e.g.*, lovastatin), marine organisms (*e.g.*, bryostatins) and plants (*e.g.*, macrocyclic musks), exhibiting a breadth of biological activities and applications.<sup>1</sup> A rare but synthetically intriguing sub-class is chlorinated macrolactones,<sup>2</sup> found in marine organisms or microbial symbionts of sponges, bryozoans and tunicates, where

halogenating enzymes are operative, and where the host organism is believed to employ such compounds as anti-foulants or chemical defenses against predators.<sup>3</sup> The interest surrounding macrolactones and the need to exploit their potential applications, has served as a major drive for the development of numerous macrocyclization strategies, which have successfully provided access to valuable macrolactones of medicinal relevance or ones finding uses as fragrances or (semi) synthetic intermediates.<sup>4</sup> Some of these methodologies have proved to be of general applicability for synthesizing additional types of macrocyclic esters, beyond macrolactones, while regioselective introduction of halogen atoms to their structure, if needed, remains synthetically challenging.

Macrocyclic esters of different types are also considered valuable in the field of materials. Most notably, macrocyclic diesters derived from the intermolecular cyclization between  $\alpha,\omega$ -alkanyldiols and malonyl dichloride have been explored extensively in the last two decades, as addends and cyclic tether systems for the controlled preparation of C<sub>60</sub> fullerene multi-adducts.<sup>5</sup> Interestingly, phenol- or catechol-derived alkynyl counterparts remain highly unusual and understudied. This provided the motivation to embark on the current project. We envisaged that malonate-based macrocyclic diesters featuring

<sup>a</sup>Department of Chemistry, University of Cyprus, 1 Panepistimiou Avenue, Aglandjia, 2109 Nicosia, Cyprus. E-mail: georgiades.savvas@ucy.ac.cy

<sup>b</sup>Department of Life Sciences, School of Sciences, European University of Cyprus, 1516 Nicosia, Cyprus

<sup>†</sup> NC, deceased, June 2023.



a 4,5-diethynylbenzene-1,2-diol motif embedded in their molecular framework, would provide uniquely enhanced conformational rigidity and directionality as addends on a C<sub>60</sub> fullerene sphere,<sup>6</sup> as opposed to the previously reported, highly flexible macrocyclic diester counterparts, obtained from  $\alpha,\omega$ -alkanyldiols. Moreover, the presence of the 1,2-diol moiety would endow our macrocycles with the potential to chelate metal cations or engage in boronic ester dynamic chemistry, a property useful for ion sensing or supramolecular chemistry applications. Therefore, the current study was initiated as an integrated synthetic effort to access unprecedented macrocyclic diesters from catechol-originating propargyl diols and malonyl dichloride.

Part of our approach was the inclusion of diverse protecting groups on catechol hydroxy sites, initially to identify optimal ones for macrocyclization efficiency, but ultimately to realize that they can also exert a role in regulating alkyne reactivity, since the alkyne sites “communicate” with the catechol substituents *via* the conjugated aromatic system. Herein, we report the occurrence of regio- and stereo-selective alkyne hydrochlorination on methoxy and silyloxy catechol-derived propargyl diols, in the course of their macrocyclization with malonyl dichloride, to form 13-membered diesters. Interestingly, unsubstituted and electron-withdrawing O-substituted, or even conformationally restricted O-substituted arylpropargyldiols, did not exhibit similar reactivity, suggesting a (stereo)electronic dependence of product distribution, which may be exploitable synthetically. The possibility of obtaining halogenated variants of such macrocyclic diesters under cyclization conditions, especially in the form of vinyl halide derivatives, may open new routes for chemical functionalization of these precious materials.

Vinyl or alkenyl halides, formally generated from hydrogen halide electrophilic addition to alkynes, are a class of useful organic intermediates that may serve as key building blocks in selected organometallic transformations, such as C–C<sup>7</sup> and C–N<sup>8</sup> cross-coupling reactions, thus contributing to the increase of skeletal or functional complexity. Alkenyl halides are also frequently encountered motifs in biologically active marine natural products.<sup>9</sup> Therefore, new methodologies for their preparation constitute an expansion of the synthetic chemist's toolbox for attaining these challenging motifs.

The last decade has seen a surge of organic methodology for hydrogen halide addition to alkynes, including employing *in situ*-formed hydrogen halides or surrogates on triple bonds of arylacetylenes, leading to aryl-comprising alkenyl halides. Interestingly, the majority of new methods have heavily relied on the use of precious metal catalysts and, in some protocols, high temperatures, to carry out such transformations, including heterogeneous Au–TiO<sub>2</sub> nanoparticles,<sup>10</sup> Cp<sup>\*</sup>RuCl(cod),<sup>11</sup> RuCl<sub>2</sub>(*p*-cymene)<sub>2</sub>,<sup>12</sup> JohnPhosAuCl<sup>13</sup> or other LAuCl catalyst,<sup>14</sup> Pd(OAc)<sub>2</sub>,<sup>15</sup> and IrCl(cod)<sub>2</sub>,<sup>16</sup> due to the ability of such methods to achieve considerable stereoselectivity.

Moreover, transition metal-free conditions are traditionally known for hydrogen halide addition to arylalkynes, including TFA and halide salt combination<sup>17</sup> and CH<sub>2</sub>Br<sub>2</sub> in *N,N*-dimethylaniline.<sup>18</sup> However, it should be noted that only

a minuscule number of studies on arylalkyne hydrohalogenation, which cannot be considered systematic, have investigated the influence of strongly electron-donating substituents on the aryl ring, placed *ortho*- or *para*-relative to the alkyne substituent. In agreement with the findings of the current study, these report an enhancement of alkyne reactivity towards hydrohalogenation. Specifically, phenol-derived alkynes have been reported to afford high to excellent yields in hydrohalogenations in polar solvents,<sup>19</sup> known to stabilize charged intermediates. Aniline-derived alkynes have demonstrated similar reactivity in a recent synthetic study, supported by computational mechanistic analysis.<sup>20</sup> Herein, we further highlight interesting mechanistic aspects and considerations, arising from alkyne hydrochlorination that takes place in the course of macrocyclization, attempting to link the two events in the light of the variable aryl substituent effects.

Interestingly, direct addition of corrosive hydrogen halide to alkyne precursors in natural and other sensitive product syntheses may prove challenging, since functional group tolerance is critically important, as implied by the need for indirect generation of alkenyl halides from alkenyl stannanes<sup>21</sup> or alkenyl indanes.<sup>22</sup> For this reason, our methodology may provide alternative access to challenging macrocyclic ester targets that comprise alkenyl halide functionality.

## Results and discussion

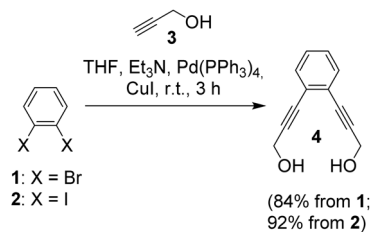
### Synthesis of a series of aryl- or catechol-derived propargyl diols

Five (5) aryl or catechol-derived propargyl diols were synthesized *via* short routes, representing a distinct class of substrates poised for macrocyclization with malonyl dichloride, to form the corresponding 13-membered diesters. Aiming to investigate the effect of the presence and nature of O-atom-based substituents on the reactivity of these diols towards the reaction with malonyl dichloride, we employed diverse protecting groups for the catecholic hydroxy groups. These included trifluoromethanesulfonyl (Tf), cyclohexylketone, methyl (Me) and *tert*-butyldimethylsilyl (TBDMS). The O-substituent-free counterpart, the simple aryl-propargyl diol, was also included in the study, to allow comparison. The selected substituent types cover a range of electronic or stereoelectronic contributions of the substituent to the bisalkyne conjugated system, thus altering its ability to undergo hydrochlorination in the course of macrocyclization and creating potential for regulating the reactivity of the diols as desired.

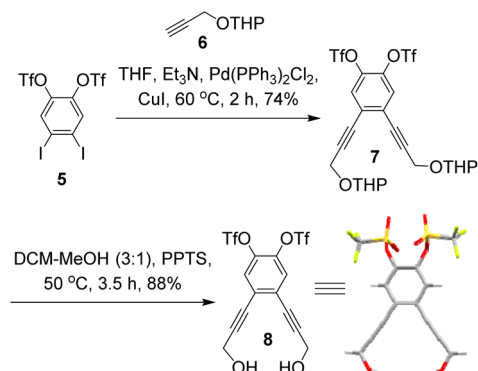
The simplest diol in the series, 3,3'-(1,2-phenylene)bis(prop-2-yn-1-ol) (**4**), featuring a hydroxy-free aryl rather than a catechol ring system, was generated from 1,2-dibromo- or the superior 1,2-diiodobenzene (**1** and **2**, respectively) and propargyl alcohol (**3**), under standard Sonogashira C–C cross-coupling conditions,<sup>23</sup> in excellent yields (Scheme 1, 84% and 92%, respectively).

Next, a catechol-derived propargyl diol, with the catecholic hydroxy groups protected in the form of trifluoromethanesulfonate esters, was generated (Scheme 2). Triflate substituents are known to inductively confer electron-





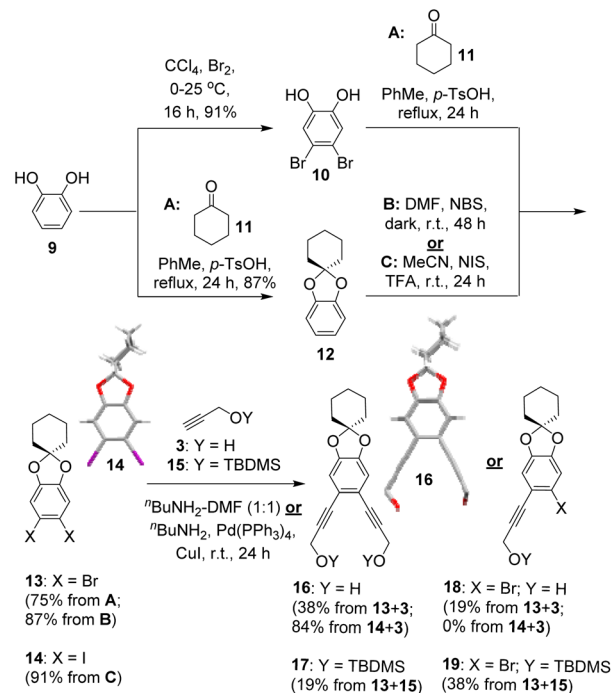
Scheme 1 Synthesis of 3,3'-(1,2-phenylene)bis(prop-2-yn-1-ol) (4).



Scheme 2 Synthetic route for accessing 4,5-bis(3-hydroxyprop-1-yn-1-yl)-1,2-phenylene bis(trifluoromethanesulfonate) (8). XRD crystal structure of compound 8 is represented as capped stick model [color code: C = grey; H = white; O = red; S = yellow; F = light green].

withdrawing properties, thus down-regulating the reactivity of the resulting conjugated substrate towards electrophilic additions. The two-step synthesis initiated from the commercially available 4,5-diiodo-1,2-phenylene bis(trifluoromethanesulfonate) (5), which was first submitted to alternative Sonogashira C–C cross-coupling conditions. In this case, tetrahydropyran (THP)-protected propargyl alcohol (6) had to be employed, while Pd(PPh<sub>3</sub>)<sub>2</sub>Cl<sub>2</sub> played the role of catalyst, at elevated temperature, to offset the moderate reactivity exhibited by substrate 5. The C–C cross-coupling afforded THP-protected diol 7 (74%), which was subsequently deprotected under acidic conditions (pyridinium *p*-toluenesulfonate, PPTS) in a mixed solvent (DCM-MeOH, 3 : 1) to afford diol 8 in 88% yield.

For the production of a cyclohexyl-protected catechol-based propargyl diol, in the form of dioxolane (16), several alternative routes were explored, to identify the most efficient one that was amenable to scale-up. Starting from simple catechol (9), conversion to 4,5-dibromobenzene-1,2-diol (10, 91%) was achieved, by applying a bromination protocol involving Br<sub>2</sub> in CCl<sub>4</sub> (Scheme 3).<sup>24</sup> This was followed by ketal protection of dibromide 10, using cyclohexanone (11) in the presence of an acid catalyst (*p*-TsOH) (method A, Scheme 3),<sup>25</sup> which generated 4,5-dibromo spiro cyclohexyl dioxolane 13 in good yield (75%), on a 0.5 g reaction scale. However, upon scale-up to 5 g, the protection reaction afforded considerably lower yield of the expected product. Therefore, an alternative route was devised, that reversed the sequence of catechol halogenation and ketal protection steps. This involved protection of catechol 9 to spiro cyclohexyl dioxolane 12 (87%) first, *via* condensation with

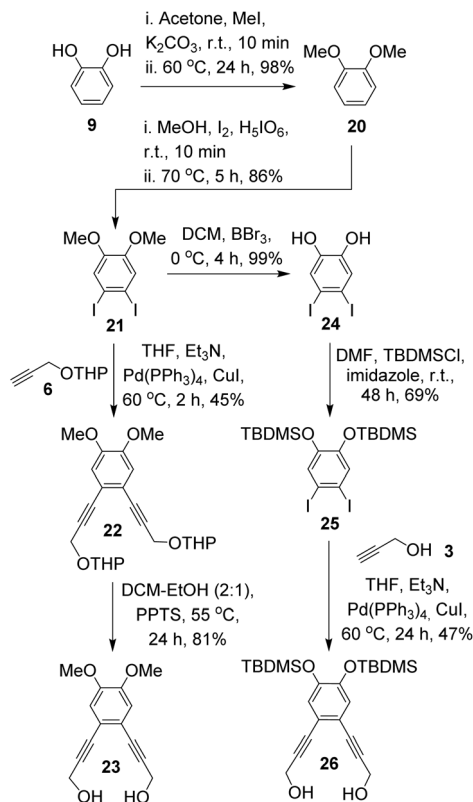


Scheme 3 Synthetic routes explored for accessing 3,3'-(spiro[benzo[d][1,3]dioxole-2,1'-cyclohexane]-5,6-diyl)bis(prop-2-yn-1-ol) (16), related 3-(5-bromospiro[benzo[d][1,3]dioxole-2,1'-cyclohexane]-6-yl)prop-2-yn-1-ol (18) and their TBDMS-protected variants (17 and 19, respectively). XRD crystal structures of compounds 14 and 16 are represented as capped stick model [color code: C = grey; H = white; O = red; I = magenta].

cyclohexanone 11 (method A), followed by halogenation to obtain a 4,5-bis-halogenated derivative of the cyclohexyl dioxolane. Two alternative methods were employed to halogenate intermediate 12. Method B (Scheme 3) employed *N*-bromosuccinimide (NBS) in DMF under darkness, at ambient temperature for 48 h, to afford spiro cyclohexyl dioxolane 13, in 87% yield. This route provided a way to efficiently generate 13 in high yields, at a large scale. However, the incomplete incorporation of propargyl alcohol 3 or TBDMS-protected propargyl alcohol 15 in the ensuing Sonogashira C–C cross-coupling with dibromide 13, which afforded monoadducts 18 (X = Br; Y = H) and 19 (X = Br; Y = TBDMS), respectively, alongside bis-propargyl alcohol 16 or protected form 17, prompted us to turn to an alternative protocol. Halogenation method C (Scheme 3) employed *N*-iodosuccinimide (NIS) in acetonitrile in the presence of TFA to deliver 4,5-diiodide 14, rather than the dibromide, in 94% yield. The reactivity of diiodide 14 in the oxidative addition step of the Sonogashira in *n*-butylamine was considerably higher than that of dibromide 13, in the case of combination with propargyl coupling partner 3, thus leading to the desired diol 16 (84%), as the only isolated Sonogashira product.

To obtain O-substituents with electron-donating properties, an additional synthetic pathway was developed (Scheme 4). Catechol (9) was converted to a dimethyl derivative (20) in near-quantitative yield (98%), upon reaction with MeI under basic conditions in acetone.<sup>26</sup> Conversion of compound 20 to a 4,5-





Scheme 4 Synthetic routes explored for accessing 3,3'-(4,5-dimethoxy-1,2-phenylene)bis(prop-2-yn-1-ol) (**23**) and 3,3'-(4,5-bis(*tert*-butyldimethylsilyloxy)-1,2-phenylene)bis(prop-2-yn-1-ol) (**26**).

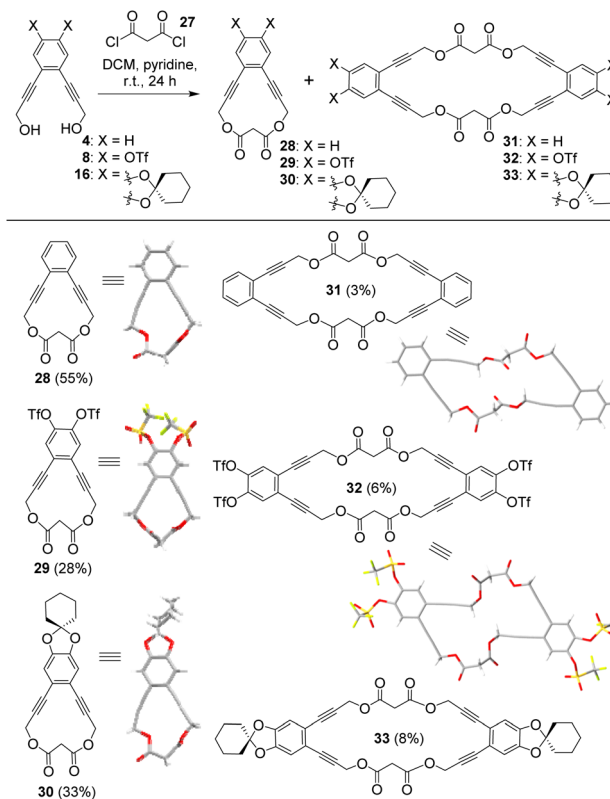
diiodo-derivative (**21**, 86%) was achieved by treating with a mixture of iodine and periodic acid in refluxing MeOH.<sup>27</sup> Conversion of diiodide **21** to a bis-alkynyl derivative (**22**), was carried out *via* Sonogashira cross-coupling, with THP-protected propargyl alcohol (**6**), at elevated temperature, to afford the product in modest yield (45%). A dimethyl-protected propargyl diol (**23**) was obtained in high yield (81%), *via* acidic deprotection (PPTS) of the THP precursor. This route was further expanded to allow the generation of a bis-TBDMS-protected propargyl diol (**26**). Diiodo-intermediate **21** had the methyl groups quantitatively removed, upon treatment with  $\text{BBr}_3$ , to afford diiodo-catechol **24**.<sup>27,28</sup> This was re-protected with TBDMS-chloride in DMF under basic conditions (imidazole) to afford intermediate **25** (69%).<sup>28</sup> Sonogashira C–C cross-coupling of diiodide **25** with propargyl alcohol **3** afforded modest yields (47%) of diol **26**.

### Synthesis of macrocyclic esters and hydrochlorinated adducts

The obtained aryl- or catechol-derived propargyl diols **4**, **8**, **16**, **23** and **26** were individually submitted to macrocyclization conditions with malonyl dichloride (**27**) in dry DCM, in the presence of pyridine base, at high dilution, as devised by Chronakis *et al.*,<sup>5b</sup> to enhance macrocycle formation. In these cases, the simple aryl (**4**), the bis-triflate (**8**) and the cyclohexylketal-based propargyl diol afforded the corresponding 13-membered macrocyclic diesters (**28** at 55%, **29** at 28%

and **30** at 33% yield, respectively), accompanied by modest amounts (3–8%) of dimeric 26-membered macrocyclic tetraesters (**31**, **32** and **33**, respectively), resulting from a 2 : 2 stoichiometry (Scheme 5). It is noteworthy that in these three cases, no indication of electrophilic addition to a triple bond was evident. We believe that in the case of the EWG (triflate), inductive electron withdrawing effect of the protecting group<sup>29</sup> reduces the nucleophilicity of the triple bond towards electrophiles, significantly lower than that of the oxygen-free substrate, where no hydrochlorination is observed either. In the case of the cyclohexylketal-based propargyl diol, the constraints imposed by the cyclohexane ring are expected to prevent alignment of oxygen atom lone pairs with the aromatic,<sup>30</sup> thus preventing triple bond nucleophilicity enhancement by means of conjugation. XRD crystal structures were obtained for all three 13-membered macrocyclic diesters in this set (**28–30**), as well as two of the 26-membered macrocyclic tetraesters (**31** and **32**), thus confirming the structures assigned by NMR spectroscopy.

On the contrary, in the electron-donating (dimethyl- and bis-TBDMS-protected) cases, the obtained product mixtures involved considerable percentages of hydrochloride adducts to a triple bond (Scheme 6). This can be attributed to  $p$ - $\pi$



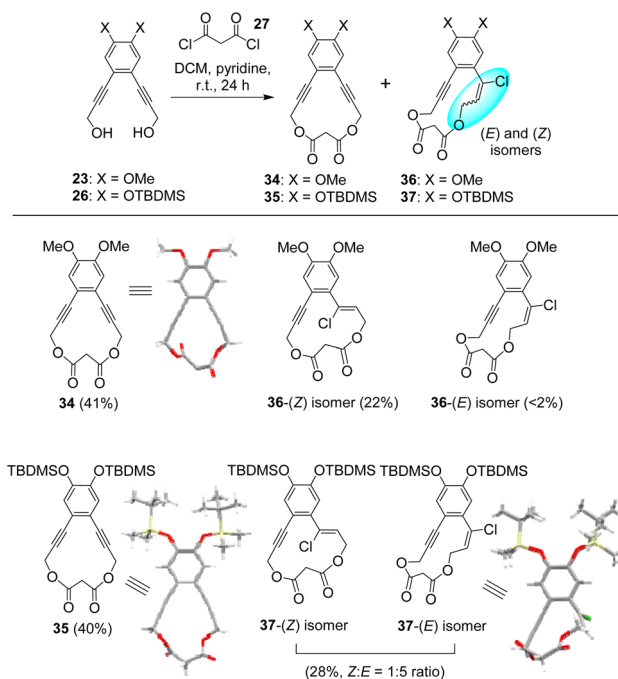
Scheme 5 Macrocyclization of aryl- or catechol-derived propargyl diols **4**, **8** and **16** with malonyl dichloride (**27**) leads to 13-membered diesters (**28**, **29** and **30**, respectively) and modest amounts of 26-membered tetraesters (**31**, **32** and **33**, respectively). XRD crystal structures of compounds **28–32** are represented as capped stick model [color code: C = grey; H = white; O = red; S = yellow; F = light green].



conjugation of the oxygen atom of the –OMe or –OTBDMS substituents with the aromatic system, increasing electron density at the *ortho* and *para* positions of the aromatic ring. Since the alkyne moieties are connected *para* relative to the catechol oxygen atoms, extended conjugation is possible, leading to an enhancement of electron density at the triple bond terminal carbon atom, thus increasing its nucleophilic capacity towards protonation. Specifically, propargyl diol **23** afforded 13-membered diester **34** (41%) under the same cyclization conditions, alongside two stereoisomeric HCl adducts, **36-(Z)** and **36-(E)**. The structure of the major isolated hydrochlorinated adduct in this case (obtained at 22% yield) was assigned as **36-(Z)**, by means of direct comparison and matching of its original <sup>1</sup>H NMR spectrum (both chemical shifts and multiplicities) to a simulated <sup>1</sup>H NMR spectrum of the (*Z*)-isomer, generated in SPARTAN<sup>24</sup>, using model ωB97X-D/6-31G\*. The original <sup>1</sup>H NMR spectrum of the minor stereoisomer (only obtained in traces <2%, assigned as **36-(E)**), featured significantly different chemical shifts and higher multiplicities for the vinylic, allylic, propargylic and malonic signals, that did not match the simulated spectra for either stereoisomer, thus suggesting magnetically nonequivalent protons within each set, presumably owing to significant conformational restriction and closer transannular contact between the propargylic, allylic and malonic fragments, as compared to its stereoisomer.

Similarly, propargyl diol **26** afforded 13-membered diester **35** (40%) under the macrocyclization conditions, alongside two

stereoisomeric HCl adducts to a triple bond (**37-(Z)** and **37-(E)**) (Scheme 6). However, in this case, a stereoselectivity switch was detected, as it was now the major stereoisomer that exhibited a higher multiplicities pattern in <sup>1</sup>H NMR, identical to that observed for the (*E*)-isomer in the previous case, in the region of vinylic, allylic, propargylic and malonic signals. Thus, the major stereoisomer was assigned as **37-(E)**. Similarly, the minor stereoisomer, assigned as **37-(Z)**, afforded multiplicities pattern similar to that of compound **36-(Z)**. The two hydrochlorinated adducts from diol **26** were obtained in 1 : 5 (*Z*)/(*E*) molar ratio, as an inseparable mixture, and added up to 28% yield. Whether this switch in stereoselectivity, as compared to the -OMe case, is a result of steric effects imposed by the bulky TBDMS protecting groups on the (*in situ*-generated) HCl (or surrogate) addition, or is connected to a (reversible) migratory behaviour of silicon between the catecholic and propargylic oxygen sites under the nucleophilic conditions of this reaction, remains to be investigated and will serve as the object of future mechanistic work. A crystallization attempt from the mixture of the two stereoisomers was undertaken, which successfully afforded crystalline material, used for X-ray diffraction (XRD) studies. The solved structure was found to correspond to the major isomer, **37-(E)**. XRD crystal structures were also obtained for both non-hydrochlorinated 13-membered diesters, **34** and **35**. Altogether, the distribution of products in the macrocyclization of propargyl diols with malonyl dichloride, under basic conditions, appears to be dependent on the substitution pattern of the aromatic ring, a system that electronically “cross-talks”, by means of conjugation, with the bis-propargyl diol functionality. The dual behavior of the examined propargyl diols, *i.e.*, predisposition or lack thereof for electrophilic addition, implies an electronic and/or stereoelectronic effect of the catechol O-substituent on the reactivity of the propargyl system's triple bonds. The absence of bis hydrochloride adducts in the last two cases may imply a prohibition imposed by macrocyclic ring strain, at the mono-adduct stage, on a second HCl addition.



**Scheme 6** Macrocyclization of catechol-derived propargyl diols **23** and **26** with malonyl dichloride (**27**) leads to 13-membered diesters (**34** and **35**, respectively) and mono-hydrochlorination derivatives (**36** and **37**, respectively), as isomeric (*Z*)/(*E*) mixtures. XRD crystal structures of compounds **34**, **35** and **37-(E)** are represented as capped stick model [color code: C = grey; H = white; O = red; Si = light yellow; Cl = green].

### Control experiments to provide mechanistic insights

Genuinely intrigued by the results and product distributions obtained with the malonyl dichloride/pyridine/anhydrous DCM conditions, we have designed a series of control experiments that involve absence of malonyl dichloride or pyridine base, aiming to obtain mechanistic insight, specifically to identify the form in which the *in situ*-generated HCl (or surrogate) is delivered to the triple bond in the original reaction, as well as to assess the effect of reaction conditions (basic vs. acidic) and possibly the influence of macrocyclic ring strain (*vs.* the open diol) on triple bond reactivity in these systems. The control experiments compared two substrates, the non-cyclized methoxy (–OMe) – substituted diol **23** *vs.* the related 13-membered macrocyclic diester **34**, and two alternative sets of conditions that involved pyridinium hydrochloride (equimolar to the substrate or in 5-fold excess) *vs.* freshly prepared HCl gas (introduced *via* bubbling for 4 h, in >100-fold excess relative to the substrate), in halogenated solvent (anhydrous dichloromethane or chloroform), in the absence of free pyridine,



at room temperature. Pyridinium hydrochloride may occur as a by-product in the original reaction mix of propargyl diol, pyridine and malonyl dichloride, which could be responsible for HCl delivery to the triple bond. Alternatively, *in situ*-generated HCl could be adding directly, without the mediation of pyridine. In fact, one additional experiment, under the original macrocyclization conditions of **23** to **34**, but in the absence of pyridine or other base, showed that cyclization could still proceed to afford macrocycle **34** to a considerable extent (32%). All studied control combinations are shown in Scheme 7.

Interestingly, only the non-cyclized diol, **23**, allowed (double) hydrochlorination to afford **38** (as a mixture of three stereoisomers, of which one was dominant and the other two only appeared in traces) (Scheme 7). This may imply that, in the case of macrocyclic substrate **34**, a potential loss of triple bond linearity and rearrangement to the bulkier, more transannularly-strained vinyl chloride, due to the HCl addition, could be a kinetically slow and unfavourable process. This hypothesis, although consistent with the extensive rearrangements that have to take place in the molecule during the transformation, would require further support from computational calculations of transition states. Notably, only HCl gas led to reaction, while use of pyridinium hydrochloride as the form of HCl delivery, even at 5-fold excess and over a prolonged period of time, did not yield any electrophilic addition product, indicating that pyridine-associated HCl is an unlikely source of HCl in the original reaction. Taken together, these findings may provide an indication of the sequence of elementary steps taking place in the original reaction with malonyl dichloride under the basic conditions (Scheme 6). Specifically, they suggest

that HCl electrophilic addition to a triple bond likely occurs prior to macrocyclization, while HCl could be released from malonyl dichloride upon attack by the first alcohol and potentially react with the triple bond without the mediation of pyridine.

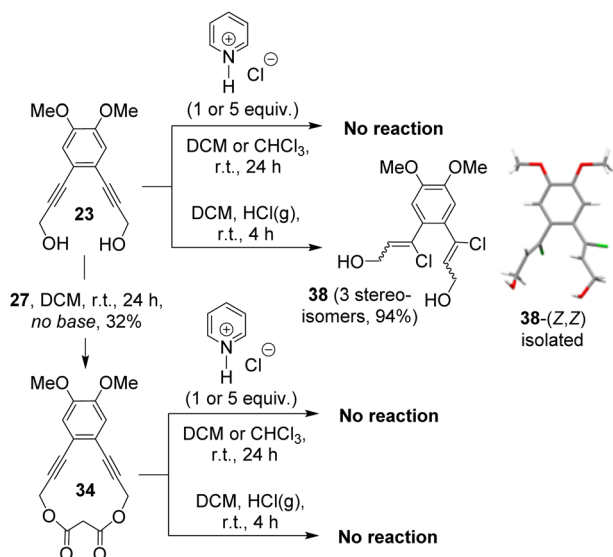
### Crystal packing of synthesized macrocyclic esters

X-ray diffraction (XRD) crystallographic studies have revealed the crystal packing of the aryl- and catechol-derived alkynyl dimeric 26-membered tetraesters **31** and **32**, respectively, which interestingly exhibit a columnar arrangement of neighbouring molecules to form tubular assemblies, as shown in Fig. 1. Notably, a similar type of assembly has been reported in the past for a series of more flexible, but smaller in ring size, macrocyclic tetraesters, formed from  $\alpha,\omega$ -alkanyldiols and malonyl dichloride.<sup>5b</sup>

## Experimental

### General methods and instrumentation

Reagent grade chemicals (purity >97%) were obtained from commercial sources, such as Sigma-Aldrich (St. Louis, MO, USA), Alfa Aesar (Haverhill, MA, USA) and TCI Europe N.V. (Zwijndrecht, Belgium), and used without further purification. Organic solvents used for reactions, obtained from Carlo Erba Reagents (Milano, Italy), were anhydrous unless otherwise stated. Organic solvents used for chromatography, obtained from Merck (Burlington, MA, USA), were of analytical grade. All synthetic procedures were conducted under inert atmosphere, unless otherwise specified. Flash chromatographic purifications were performed in glass columns, using silica gel 60 (0.063–0.2 mm) from Merck as the stationary phase. Thin layer chromatography (TLC), to monitor reaction progress, was performed on aluminum plates covered with silica gel 60 (F254) from Merck, which allowed compound visualization under a UV lamp (254 nm) as dark spots on a green background. TLC staining was performed with vanillin (TCI Europe N.V.) where necessary. Nuclear magnetic resonance (NMR) spectra were obtained on a Bruker Avance III 500 Ultrashield Plus spectrometer (at 500 MHz for <sup>1</sup>H NMR and 125 MHz for <sup>13</sup>C NMR, at 25 °C). Chemical shift calibration was based on the NMR



**Scheme 7** Control experiments for the investigation of the HCl form of delivery in the macrocyclization reaction and the assessment of the effect of reaction conditions and macrocyclic ring strain (or lack thereof) on triple bond reactivity. Only open diol **23** allowed (double) hydrochlorination product formation, upon reaction with HCl gas in DCM. [The HCl gas was produced by reaction of NaCl(s) with concentrated sulfuric acid (99.999% wt.) at 200 °C and dried by passing it through an anhydrous CaCl<sub>2</sub>-filled column prior to use].

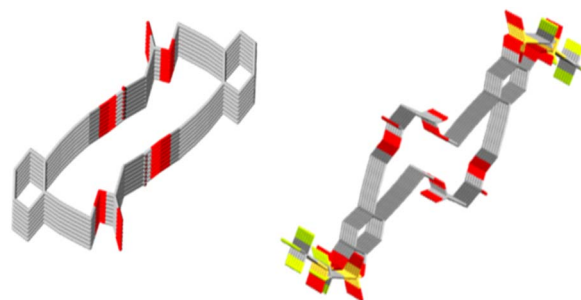


**Fig. 1** Columnar arrangements of 26-membered macrocyclic tetraesters **31** (left, top view) and **32** (right, side view) in the crystal, as per X-ray diffraction crystallographic studies, to form tubular assemblies. [color code: C = grey; O = red; S = yellow; F = light green].



solvent's residual peak. Deuterated solvents were obtained from Merck or TCI Europe N.V. Detailed synthetic procedures for new compounds are described in the SI.

### X-ray diffraction (XRD) studies

Single crystal X-ray diffraction data for compounds **8**, **28**, and **31** were collected on a XtaLAB Synergy, single source at home/near, HyPix diffractometer, equipped with a CCD area detector utilizing Cu-K $\alpha$  radiation ( $\lambda = 1.5418 \text{ \AA}$ ). Data for the rest of the compounds that afforded suitable crystals were collected on an Oxford-Diffraction Supernova diffractometer, equipped with a CCD area detector utilizing Cu-K $\alpha$  radiation ( $\lambda = 1.5418 \text{ \AA}$ ) (for compounds **14**, **16**, **29**, **30**, **32**, **34**, **37-(E)** and **38-(Z,Z)**) and Mo-K $\alpha$  radiation ( $\lambda = 0.71073 \text{ \AA}$ ) (for compound **35**). The process involved attachment of suitable crystals to glass fibers using paratone-N oil and transfer to a goniostat, where they were cooled for data collection. Unit cell dimensions were determined and refined. Empirical absorption corrections (multi-scan based on symmetry-related measurements) were applied using CrysAlis RED software [CrysAlis CCD and CrysAlis RED, version 1.171.32.15; Oxford Diffraction Ltd, Abingdon, Oxford, England, 2008]. The structures of compounds **16**, **32**, **35** and **38-(Z,Z)** were solved by direct method and refined on F2 using full-matrix least squares in SHELXL97.<sup>31</sup> The following software packages were used: CrysAlis CCD1 for data collection; CrysAlis1 for cell refinement and data reduction; WINGX<sup>32</sup> for geometric calculations; and DIAMOND [DIAMOND, version 3.1d; Brandenburg, K., Crystal Impact GbR, Bonn, Germany, 2006] for molecular graphics. Structures **8**, **14**, **28**, **29**, **30**, **31**, **34** and **37-(E)** were solved using Olex2,<sup>33</sup> with the olex2.solve structure solution program<sup>34</sup> using Charge Flipping, and refined with the SHELXL refinement package<sup>35</sup> using least squares minimization. The non-hydrogen (H) atoms were treated anisotropically. The hydrogen (H) atoms were placed in calculated, ideal positions and refined as riding on their respective carbon (C) atoms. To limit the disorder of functional groups or lattice solvent molecules, various restraints have been applied in the refinement of the crystal structures. All the crystal structures described in this study were deposited *via* the joint CCDC/FIZ Karlsruhe deposition service and have been assigned the following deposition numbers (CCDC): **8**-2423950, **14**-2423960, **16**-2423951, **28**-2424604, **29**-2423957, **30**-2423952, **31**-2423953, **32**-2423958, **34**-2423956, **35**-2423954, **37-(E)**-2423955, **38-(Z,Z)**-2423959.

## Conclusions

The investigated aryl- or catechol-derived propargyl diol reaction with malonyl dichloride under basic conditions, denotes a dependence of triple bond ability to undergo electrophilic addition, on the nature and (stereo)electronic properties of the individual aryl substituents. The connectivity of O-based substituents, *para* to the triple bonds, allows them to impact triple bond reactivity, either inductively or conjugatively. The absence of O-substitution, and likewise presence of a (inductively) strong electron-withdrawing protecting group (Tf) on the

catechol O-atoms, renders the propargyl system's triple bonds rather unreactive toward *in situ*-generated HCl, thus favouring the simple and unmodified macrocyclization product, a 13-membered diester, and traces of a larger, 2 : 2 macrocycle, a 26-membered tetraester. In the case of a cyclohexyl-ketal derivative, while also not affording HCl adducts, the absence of electrophilic addition to triple bonds can be attributed to the restricted ability of the substituent's O-atoms to effectively engage in conjugation with the aryl ring's  $\pi$ -system. Replacing one of these protecting groups with one that allows efficient donation of electron density from the O-atoms to the aryl ring's  $\pi$ -system, such as methyl or *tert*-butyldimethylsilyl, leads to an alteration of reactivity to one that allows the propargyl triple bond to form valuable HCl adducts. Mechanistically, control experiments have suggested *in situ*-generated HCl, rather than pyridine-sequestered HCl, as the form in which HCl is delivered to the triple bond in the hydrochlorination reaction, and have provided useful insights on the series of elementary steps involved. The rather diverging stereoselectivity preference of the tested substrates (**23** vs. **26**) in the addition mode of HCl during macrocyclization, characterised as *anti* and *syn*, respectively, is possibly related to the unique structural features and properties of each O-atom protecting group. An effort to further investigate this dual behaviour, both synthetically and computationally, is already under way in our laboratory. It is anticipated to help elucidate the mechanistic details and stereoselectivity origins for diverse cases, and to enable decision-making about how these systems could be maximally exploited in a synthetic context. In summary, it has been shown that the efficient pairing of catechol systems with propargyl systems can lead to new reactivities, that could be fine-tuned by the choice of aryl substituents on the aromatic, revealing interesting mechanistic knowledge, while providing access to new unsaturated halogenated organic macrocyclic intermediates, difficult to attain by alternative methods. Future synthetic directions of this project could focus on further developing reaction conditions to render alkyne hydrohalogenation leading to macrocyclic vinyl halides the dominant transformation. On the front of exploring various practical implications of this work, determining binding affinities of these macrocycles for physiologically relevant cations (*e.g.*, Na<sup>+</sup>, K<sup>+</sup>)<sup>36</sup> could be useful for ion sensing, while exploring transition metal cation complexation ability of the 1,2-diol moiety of the compounds could provide a platform for supra-molecular self-assembly.

## Author contributions

GL: compound synthesis and characterization, crystal growing, data collection, processing and interpretation, manuscript draft writing; AK: XRD data collection and processing, manuscript draft writing; NC: project supervision, reaction design; SNG: project supervision, reaction design, data interpretation, final manuscript writing.

## Conflicts of interest

There are no conflicts to declare.



## Data availability

CCDC 8-2423950, 14-2423960, 16-2423951, 28-2424604, 29-2423957, 30-2423952, 31-2423953, 32-2423958, 34-2423956, 35-2423954, 37-(E)-2423955 and 38-(Z,Z)-2423959 contain the supplementary crystallographic data for this paper.<sup>37a-1</sup>

The data supporting this article have been included as part of the supplementary information (SI). Supplementary information: synthetic methods and characterization data; <sup>1</sup>H, <sup>13</sup>C and <sup>19</sup>F NMR spectra of synthesized compounds; <sup>1</sup>H NMR simulations of selected chlorinated adducts; Single-crystal X-ray diffraction data. See DOI: <https://doi.org/10.1039/d5ra09108j>.

## Acknowledgements

We acknowledge the University of Cyprus for supporting this project through allocation of public funding.

## Notes and references

- (a) G. P. Dinou, The macrolide antibiotics renaissance, *Br. J. Pharmacol.*, 2017, **174**, 2967; (b) R. Raghuvanshi and S. B. Bharate, Preclinical and clinical studies on bryostatins, a class of marine-derived protein kinase C modulators: A mini-review, *Curr. Top. Med. Chem.*, 2020, **20**, 1124; (c) E. S. El-khayat, M. E. Abouelela, R. A. Abdelhamid, M. S. Alorainy and K. A. Shaaban, Macrolactones and macrolides from plant endophytic fungi, chemical scaffolds, biological activities and spectroscopy: A comprehensive review, *Bull. Pharm. Sci.*, 2024, **47**, 151; (d) M. A. M. Mondol, H. J. Shin and M. T. Islam, Diversity of secondary metabolites from marine *Bacillus* species: chemistry and biological activity, *Mar. Drugs*, 2013, **11**, 2846.
- (a) D. S. Dalisay, B. I. Morinaka, C. K. Skepper and T. F. Molinski, A tetrachloro polyketide hexahydro-1*H*-isoindolone, muironolide A, from the marine sponge *Phorbas* sp. Natural products at the nanomole scale, *J. Am. Chem. Soc.*, 2009, **131**, 7552; (b) S. La Barre, P. Potin, C. Leblanc and L. Delage, *Mar. Drugs*, 2010, **8**, 988.
- (a) J.-A. Kim, S.-S. Choi, J. K. Lim and E.-S. Kim, Unlocking marine treasures: isolation and mining strategies of natural products from sponge-associated bacteria, *Nat. Prod. Rep.*, 2025, **42**, 1195; (b) T. R. A. Thomas, D. P. Kavlekar and P. A. LokaBharathi, Marine Drugs from Sponge-Microbe Association—A Review, *Mar. Drugs*, 2010, **8**, 1417.
- (a) M. van Hoof, G. Force and D. Leboeuf, Modern macrolactonization techniques, *Synthesis*, 2024, **56**, 714; (b) J. Guerrero-Morales and S. K. Collins, Biocatalysis as a versatile tool for macrolactonization: comparative evaluation of catalytic and stoichiometric approaches, *Green Chem.*, 2024, **26**, 10404; (c) R. S. Brzozowski and W. M. Wuest, Twelve-membered macrolactones: privileged scaffolds for the development of new therapeutics, *Chem. Biol. Drug Des.*, 2017, **89**, 169; (d) Y. Li, X. Yin and M. Dai, Catalytic macrolactonizations for natural product synthesis, *Nat. Prod. Rep.*, 2017, **34**, 1185; (e) X. Wu and D. Sun, Macrocyclic drugs and synthetic methodologies toward macrocycles, *Molecules*, 2013, **18**, 6230.
- (a) U. Reuther, T. Brandmüller, W. Donaubaue, F. Hampel and A. Hirsh, A highly regioselective approach to multiple adducts of C60 governed by strain minimization of macrocyclic malonate addends, *Chem. Eur. J.*, 2002, **8**, 2261; (b) N. Chronakis, T. Brandmüller, C. Kovacs, U. Reuther, W. Donaubaue, F. Hampel, F. Fisher, F. Diederich and A. Hirsh, Macrocyclic cyclo[*n*]malonates – Synthetic aspects and observation of columnar arrangements by X-ray crystallography, *Eur. J. Org. Chem.*, 2006, **2006**, 2296; (c) W. Yan, S. M. Seifermann, P. Pierrat and S. Bräse, Synthesis of highly functionalized C60 fullerene derivatives and their applications in material and life sciences, *Org. Biomol. Chem.*, 2015, **13**, 25; (d) F. Schillinger, U. Hahn, S. Guerra, T. M. N. Trinh, D. Sigwalt, M. Holler, I. Nierengarten and J.-F. Nierengarten, Si-tethered bis- and tris-malonates for the regioselective preparation of fullerene multi-adducts, *Helv. Chim. Acta*, 2023, **106**, e202300026.
- G. Lefkaritis, A. Kourtellaris, N. Chronakis and S. N. Georgiades, manuscript in preparation.
- (a) W. Wu and H. Jiang, Haloalkynes: A powerful and versatile building block in organic synthesis, *Acc. Chem. Res.*, 2014, **47**, 2483; (b) C. C. C. Johansson Seechurn, M. O. Kitching, T. J. Colacot and V. Snieckus, Palladium-catalyzed cross-coupling: a historical contextual perspective to the 2010 Nobel Prize, *Angew. Chem., Int. Ed.*, 2012, **51**, 5062.
- (a) J. F. Hartwig, Evolution of a fourth generation catalyst for the amination and thioetherification of aryl halides, *Acc. Chem. Res.*, 2008, **41**, 1534; (b) P. Ruiz-Castillo and S. L. Buchwald, Applications of palladium-catalyzed C–N cross-coupling reactions, *Chem. Rev.*, 2016, **116**, 12564.
- (a) J. K. Nunnery, N. Engene, T. Byrum, Z. Cao, S. V. Jabba, A. R. Pereira, T. Matainaho, T. F. Murray and W. H. Gerwick, Biosynthetically intriguing chlorinated lipophilic metabolites from geographically distant tropical marine cyanobacteria, *J. Org. Chem.*, 2012, **77**, 4198; (b) T. Akiyama, K. Takada, T. Oikawa, N. Matsuura, Y. Ise, S. Okada and S. Matsunaga, Stimulators of adipogenesis from the marine sponge *Xestospongia testudinaria*, *Tetrahedron*, 2013, **69**, 6560; (c) W.-J. Chung and C. D. Vanderwal, Stereoselective halogenation in natural product synthesis, *Angew. Chem., Int. Ed.*, 2016, **55**, 4396; (d) K. C. Nicolaou, P. G. Bulger and D. Sarlah, Palladium-catalyzed cross-coupling reactions in total synthesis, *Angew. Chem., Int. Ed.*, 2005, **44**, 4442; (e) R. Jana, T. P. Pathak and M. S. Sigman, Advances in transition metal (Pd, Ni, Fe)-catalyzed cross-coupling reactions using alkyl-organometallics as reaction partners, *Chem. Rev.*, 2011, **111**, 1417; (f) A. B. Dounay and L. E. Overman, The asymmetric intramolecular Heck reaction in natural product total synthesis, *Chem. Rev.*, 2003, **103**, 2945.
- (a) J. Oliver-Meseguer, A. Doménech-Carbó, M. Boronat, A. Leyva-Pérez and A. Corma, Partial reduction and



- selective transfer of hydrogen chloride on catalytic gold nanoparticles, *Angew. Chem., Int. Ed.*, 2017, **56**, 6435; (b) S. Liang, R. Ebule, G. B. Hammond and B. Xu, A chlorinating reagent yields vinyl chlorides with high regioselectivity under heterogeneous gold catalysis, *Org. Lett.*, 2017, **19**, 4524.
- 11 S. Dérien, H. Klein and C. Bruneau, Selective ruthenium-catalyzed hydrochlorination of alkynes: One-step synthesis of vinylchlorides, *Angew. Chem., Int. Ed.*, 2015, **54**, 12112.
  - 12 Y. Bai, Z. Lin, Z. Ye, D. Dong, J. Wang, L. Chen, F. Xie, Y. Li, P. H. Dixneuf and M. Zhang, Ruthenium-catalyzed regioselective hydrohalogenation of alkynes mediated by trimethylsilyl triflate, *Org. Lett.*, 2022, **24**, 7988.
  - 13 X. Zeng, S. Liu, G. B. Hammond and B. Xu, Hydrogen-bonding-assisted Brønsted acid and gold catalysis: Access to both (*E*)- and (*Z*)-1,2-haloalkenes via hydrochlorination of haloalkynes, *ACS Catal.*, 2018, **8**, 904.
  - 14 R. Ebule, S. Liang, G. B. Hammond and B. Xu, Chloride-tolerant gold(I)-catalyzed regioselective hydrochlorination of alkynes, *ACS Catal.*, 2017, **7**, 6798.
  - 15 G. Zhu, D. Chen, Y. Wang and R. Zheng, Highly stereoselective synthesis of (*Z*)-1,2-dihaloalkenes by a Pd-catalyzed hydrohalogenation of alkynyl halides, *Chem. Commun.*, 2012, **48**, 5796.
  - 16 P. Yu, A. Bismuto and B. Morandi, Iridium-catalyzed hydrochlorination and hydrobromination of alkynes by shuttle catalysis, *Angew. Chem., Int. Ed.*, 2020, **59**, 2904.
  - 17 H. M. Weiss, K. M. Touchette, S. Angell and J. Khan, The concerted addition of HBr to aryl alkynes; orthogonal pi bond selectivity, *Org. Biomol. Chem.*, 2003, **1**, 2152.
  - 18 X. Chen, T. Chen, Y. Xiang, Y. Zhou, D. Han, L.-B. Han and S.-F. Yin, Metal-free regioselective hydrobromination of alkynes through C-H/C-Br activation, *Tetrahedron Lett.*, 2014, **55**, 4572.
  - 19 X. Xu, C.-H. Ma, F.-R. Xiao, H.-W. Chen and B. Dai, Catalyst-free hydrochlorination protocol for terminal arylalkynes with hydrogen chloride, *Chin. Chem. Lett.*, 2016, **27**, 1683.
  - 20 H. Asahara, Y. Mukaijo, K. Muragishi, K. Iwai, A. Ito and N. Nishiwaki, Metal-free and *syn*-selective hydrohalogenation of alkynes through a pseudo-intramolecular process, *Eur. J. Org. Chem.*, 2021, **2021**, 5747.
  - 21 (a) Z. Meng, L. Souillart, B. Monks, N. Huwyler, J. Herrmann, R. Müller and A. Fürstner, A “motif-oriented” total synthesis of nannocystin ax. Preparation and biological assessment of analogues, *J. Org. Chem.*, 2018, **83**, 6977; (b) S. M. Rummelt, J. Preindl, H. Sommer and A. Fürstner, Selective formation of a trisubstituted alkene motif by *trans*-hydrostannation/Stille coupling: Application to the total synthesis and late-stage modification of 5,6-dihydrocineromycin B, *Angew. Chem., Int. Ed.*, 2015, **54**, 6241.
  - 22 M. Heinrich, J. J. Murphy, M. K. Ilg, A. Letort, J. T. Flasz, P. Philipps and A. Fürstner, Chagosensine: A riddle wrapped in a mystery inside an enigma, *J. Am. Chem. Soc.*, 2020, **142**, 6409.
  - 23 G. Just and R. Singh, The synthesis of 11-13-membered diacetylenic and 18-membered tetraacetylenic ring systems, *Tetrahedron Lett.*, 1987, **28**, 5981.
  - 24 C. F. van Nostrum, S. J. Picken, A.-J. Schouten and R. J. M. Nolte, Synthesis and supramolecular chemistry of novel liquid crystalline crown ether-substituted phthalocyanines: Toward molecular wires and molecular ionoelectronics, *J. Am. Chem. Soc.*, 1995, **117**, 9957.
  - 25 U. Drechsler, M. Pfaff and M. Hanack, Synthesis of novel functionalised zinc phthalocyanines applicable in photodynamic therapy, *Eur. J. Org. Chem.*, 1999, **1999**, 3441.
  - 26 B. Behramand, F. Molin and H. Gallardo, 2,1,3-Benzoxadiazole and 2,1,3-benzothiadiazole-based fluorescent compounds: Synthesis, characterization and photophysical/electrochemical properties, *Dyes Pigm.*, 2012, **95**, 600.
  - 27 T. J. Fisher and P. H. Dussault, Regioselective synthesis of tetraalkynylarenes by consecutive dual Sonogashira coupling reactions of the bis(triflate) of 4,5-diiodobenzene-1,2-diol, *Eur. J. Org. Chem.*, 2012, **2012**, 2831.
  - 28 J. D. Kinder and W. J. Youngs, Preparation and structural characterization of a platinum catecholate complex containing two 3-ethynylthiophene groups, *Organometallics*, 1996, **15**, 460.
  - 29 P. J. Stang and A. G. Anderson, Hammett and Taft substituent constants for the mesylate, tosylate, and triflate groups, *J. Org. Chem.*, 1976, **41**, 781.
  - 30 P. G. M. Wuts and T. W. Greene, *Green's Protective Groups in Organic Synthesis*, 4th ed., Wiley, Hoboken, NJ, 2007, pp. 367–430.
  - 31 G. M. Sheldrick, *SHELXL-97: A Program for the Refinement of Crystal Structure*, University of Göttingen, Göttingen, Germany, 1997.
  - 32 L. J. Farrugia, WinGX suite for small-molecule single-crystal crystallography, *J. Appl. Cryst.*, 1999, **32**, 837.
  - 33 O. V. Dolomanov, L. J. Bourhis, R. J. Gildea, J. A. K. Howard and H. Puschmann, OLEX2: a complete structure solution, refinement and analysis program, *J. Appl. Cryst.*, 2009, **42**, 339.
  - 34 L. J. Bourhis, O. V. Dolomanov, R. J. Gildea, J. A. K. Howard and H. Puschmann, The anatomy of a comprehensive constrained, restrained refinement program for the modern computing environment - Olex2 dissected, *Acta Crystallogr. A Found. Adv.*, 2015, **71**, 59.
  - 35 G. M. Sheldrick, SHELXT - Integrated space-group and crystal-structure determination, *Acta Crystallogr. C Struct. Chem.*, 2015, **71**, 3.
  - 36 The MALDI-TOF mass spectra of all macrocyclic esters synthesized in this study (see SI) include peaks corresponding to  $[M+Na]^+$  and/or  $[M+K]^+$ , implying an intrinsic ability of the oxygen atom-laced macrocycles for interaction with these monovalent cations.
  - 37 (a) CCDC 2423950: Experimental Crystal Structure Determination, 2026, DOI: [10.5517/ccdc.csd.cc2mc9y8](https://doi.org/10.5517/ccdc.csd.cc2mc9y8); (b) CCDC 2423960: Experimental Crystal Structure Determination, 2026, DOI: [10.5517/ccdc.csd.cc2mc9y8](https://doi.org/10.5517/ccdc.csd.cc2mc9y8); (c) CCDC 2423951: Experimental Crystal Structure Determination, 2026, DOI: [10.5517/ccdc.csd.cc2mc9y8](https://doi.org/10.5517/ccdc.csd.cc2mc9y8); (d) CCDC 2424604: Experimental Crystal Structure Determination, 2026, DOI: [10.5517/ccdc.csd.cc2mc9y8](https://doi.org/10.5517/ccdc.csd.cc2mc9y8); (e)



CCDC 2423957: Experimental Crystal Structure Determination, 2026, DOI: [10.5517/ccdc.csd.cc2mc9y8](https://doi.org/10.5517/ccdc.csd.cc2mc9y8); (f)  
CCDC 2423952: Experimental Crystal Structure Determination, 2026, DOI: [10.5517/ccdc.csd.cc2mc9y8](https://doi.org/10.5517/ccdc.csd.cc2mc9y8); (g)  
CCDC 2423953: Experimental Crystal Structure Determination, 2026, DOI: [10.5517/ccdc.csd.cc2mc9y8](https://doi.org/10.5517/ccdc.csd.cc2mc9y8); (h)  
CCDC 2423958: Experimental Crystal Structure Determination, 2026, DOI: [10.5517/ccdc.csd.cc2mc9y8](https://doi.org/10.5517/ccdc.csd.cc2mc9y8); (i)

CCDC 2423956: Experimental Crystal Structure Determination, 2026, DOI: [10.5517/ccdc.csd.cc2mc9y8](https://doi.org/10.5517/ccdc.csd.cc2mc9y8); (j)  
CCDC 2423954: Experimental Crystal Structure Determination, 2026, DOI: [10.5517/ccdc.csd.cc2mc9y8](https://doi.org/10.5517/ccdc.csd.cc2mc9y8); (k)  
CCDC 2423955: Experimental Crystal Structure Determination, 2026, DOI: [10.5517/ccdc.csd.cc2mc9y8](https://doi.org/10.5517/ccdc.csd.cc2mc9y8); (l)  
CCDC 2423959: Experimental Crystal Structure Determination, 2026, DOI: [10.5517/ccdc.csd.cc2mc9y8](https://doi.org/10.5517/ccdc.csd.cc2mc9y8).

